Short Title: Monocot ELF3 functions in dicots

Corresponding Author:

Dmitri A. Nusinow, Ph.D.
Assistant Member
Danforth Plant Science Center
975 N. Warson Rd.- Room 3030
St. Louis, MO 63132
(314)587-1489
meter@danforthcenter.org

Cross-species complementation reveals conserved functions for EARLY FLOWERING 3 between monocots and dicots

He Huang, Malia A. Gehan, Sarah E. Huss, Sophie Alvarez[2], Cesar Lizarraga, Ellen L. Gruebbling, John Gierer, Michael J. Naldrett[2], Rebecca K. Bindbeutel, Bradley S. Evans, Todd C. Mockler, and Dmitri A. Nusinow[*]

Donald Danforth Plant Science Center, St. Louis, MO, 63132, USA (H.H., M.A.G., S.A., C.L., J.G., M.J.N., R.K.B., B.S.E., T.C.M., D.A.N.)
Webster University, Webster Groves, MO, 63119, USA (S.E.H.)
Saint Louis University, St. Louis, MO, 63103, USA (E.L.G.)

One Sentence Summary:

Orthologs of a key circadian clock component ELF3 from grasses functionally complement the Arabidopsis counterpart at the molecular and physiological level, in spite of high sequence divergence.

Footnotes:

H.H., M.A.G., T.C.M., and D.A.N. conceived the project; T.C.M., B.S.E. and D.A.N. supervised the experiments; H.H., M.A.G., S.E.H., S.A., C.L., E.L.G., J.G., M.J.N., R.K.B. and D.A.N. performed the experiments; H.H., M.A.G., S.E.H., S.A., C.L., M.J.N. and D.A.N. analyzed the data; H.H., M.A.G., and D.A.N. wrote the manuscript. All authors edited the manuscript.

[1]This work was supported by the National Science Foundation (NSF) grant (IOS-1456796) to D.A.N., the NSF (DBI-0922879) grant for acquisition of the LTQ-Velos Pro Orbitrap LC-MS/MS, the U.S. Department of Energy grants (DE-SC0006627, DE-SC0012639, and DE-SC0008769) to T.C.M. and the NSF-Plant Genome grant (IOS-1202682) to M.A.G.

[2] Present addresses: University of Nebraska-Lincoln, Lincoln, NE, 68588, USA

[*]Corresponding author email: meter@danforthcenter.org

ABSTRACT

Plant responses to the environment are shaped by external stimuli and internal signaling pathways. In both the model plant *Arabidopsis thaliana* and crop species, circadian clock factors have been identified as critical for growth, flowering and circadian rhythms. Outside of *A. thaliana,* however, little is known about the molecular function of clock genes. Therefore, we sought to compare the function of *Brachypodium distachyon* and *Seteria viridis* orthologs of *EARLY FLOWERING3,* a key clock gene in *A. thaliana.* To identify both cycling genes and putative ELF3 functional orthologs in *S. viridis*, a circadian RNA-seq dataset and online query tool (Diel Explorer) was generated as a community resource to explore expression profiles of *Setaria* genes under constant conditions after photo- or thermo-entrainment. The function of *ELF3* orthologs from *A. thaliana, B. distachyon,* and *S. viridis* were tested for complementation of an *elf3* mutation in *A. thaliana.* Despite comparably low sequence identity versus AtELF3 (less than 37%), both monocot orthologs were capable of rescuing hypocotyl elongation, flowering time and arrhythmic clock phenotypes. Molecular analysis using affinity purification and mass spectrometry to compare physical interactions also found that BdELF3 and SvELF3 could be integrated into similar complexes and networks as AtELF3, including forming a composite evening complex. Thus, we find that, despite 180 million years of separation, BdELF3 and SvELF3 can functionally complement loss of *ELF3* at the molecular and physiological level.

INTRODUCTION

Plants have developed sophisticated signaling networks to survive and thrive in diverse environments. Many plant responses are shaped, in part, by an internal timing mechanism known as the circadian clock, which allows for the coordination and anticipation of daily and seasonal variation in the environment (Greenham and McClung, 2015). Circadian clocks, which are endogenous oscillators with a period of approximately 24 hours, are critical for regulating the timing of physiology, development, and metabolism in all domains of life (Bell-Pedersen et al., 2005; Doherty and Kay, 2010; Edgar et al., 2012; Harmer, 2009; Wijnen and Young, 2006). In plants and blue-green algae, circadian clocks provide an experimentally observable adaptive advantage by synchronizing internal physiology with external environmental cues (Dodd et al., 2005; Ouyang et al., 1998; Woelfle et al., 2004). Currently, circadian oscillators are best understood in the reference plant *Arabidopsis thaliana*, in which dozens of clock or clock-associated components have been identified using genetic screens and non-invasive, luciferase-based oscillating reporters (Hsu and Harmer, 2014; Nagel and Kay, 2012). These morning-, afternoon-, and evening-phased clock oscillators form multiple interconnected transcription-translation feedback loops and compose a complex network (Hsu and Harmer, 2014; Pokhilko et al., 2012). The *A. thaliana* circadian clock regulates a significant portion of physiology, including photosynthesis, growth, disease resistance, starch metabolism, and phytohormone pathways (Covington et al., 2008; Graf et al., 2010; Harmer et al., 2000; Michael et al., 2008; Wang et al., 2011b), with up to 30% of gene expression under circadian control (Covington et al., 2008; Michael et al., 2008).

Within the Arabidopsis clock network, a tripartite protein complex called the evening complex (EC) is an essential component of the evening transcription loop (Huang and Nusinow, 2016b). The EC consists of three distinct proteins, EARLY FLOWERING 3 (ELF3), EARLY FLOWERING 4 (ELF4) and LUX ARRHYTHMO (LUX, also known as PHYTOCLOCK1), with transcript and protein levels peaking in the evening (Doyle et al., 2002; Hazen et al., 2005; Hicks et al., 2001; Nusinow et al., 2011; Onai and Ishiura, 2005). The EC plays a critical role in maintaining circadian rhythms, by repressing expression of key clock genes (Dixon et al., 2011; Helfer et al., 2011; Herrero et al., 2012; Kolmos et al., 2011; Mizuno et al., 2014). Loss-of-

function mutation of any EC component in *A. thaliana* results in arrhythmicity of the circadian clock and causes excessive cellular elongation and early flowering regardless of environmental photoperiod (Doyle et al., 2002; Hazen et al., 2005; Hicks et al., 2001; Khanna et al., 2003; Kim et al., 2005; Nozue et al., 2007; Nusinow et al., 2011; Onai and Ishiura, 2005).

In *A. thaliana*, ELF3 directly interacts with ELF4 and LUX, functioning as a scaffold to bring ELF4 and LUX together (Herrero et al., 2012; Nusinow et al., 2011). Additional protein-protein interaction studies and tandem affinity purification coupled with mass spectrometry (AP-MS) have identified many ELF3-associating proteins and established ELF3 as a hub of a complex protein-protein interaction network, which consists of key components from the circadian clock pathway and light signaling pathways (Huang et al., 2016a; Huang and Nusinow, 2016b; Liu et al., 2001; Yu et al., 2008). In this network, ELF3 directly interacts with the major red light photoreceptor phytochrome B (phyB), and CONSTITUTIVE PHOTOMORPHOGENIC 1 (COP1), which is an E3 ubiquitin ligase required for proper regulation of photomorphogenesis and also interacts with phyB (Liu et al., 2001; Yu et al., 2008). The physical interaction among ELF3, phyB, and COP1, together with recruitment of direct interacting proteins to the network, provides biochemical evidence for cross-talk between circadian clock and light signaling pathways (Huang and Nusinow, 2016b). Although much work does translate from *A. thaliana* to other plant species, interaction between ELF3 and other proteins have yet to be tested in species outside *A. thaliana*. Whether evening complex-like protein assemblages or a similar ELF3-containing protein-protein interaction network exists in species outside *A. thaliana* is an interesting question to ask.

Identification and characterization of clock genes in diverse plant species has revealed that many clock components are broadly conserved (Filichkin et al., 2011; Khan et al., 2010; Lou et al., 2012; Song et al., 2010). Furthermore, comparative genomics analysis has found that circadian clock components are selectively retained after genome duplication events, suggestive of the importance of their role in maintaining fitness (Lou et al., 2012). Recently, mutant alleles of *ELF3* were identified associated with the selection of favorable photoperiodism phenotypes in several crops, such as pea, rice, soybean and barley (Faure et al., 2012; Lu et al., 2017;

Matsubara et al., 2012; Saito et al., 2012; Weller et al., 2012; Zakhrabekova et al., 2012). These findings are consistent with the reported functions of *A. thaliana* ELF3 in regulating the photoperiodic control of growth and flowering (Hicks et al., 2001; Huang and Nusinow, 2016b; Nozue et al., 2007; Nusinow et al., 2011). However, opposed to the early flowering phenotype caused by *elf3* mutants in *A. thaliana,* pea, and barley (Faure et al., 2012; Hicks et al., 2001; Weller et al., 2012), loss of function mutation of the rice or soybean *ELF3* ortholog results in delayed flowering (Lu et al., 2017; Saito et al., 2012), suggesting ELF3-mediated regulation of flowering varies in different plant species. The molecular mechanisms underlying this difference have not been thoroughly elucidated.

Brachypodium distachyon is a C3 model grass closely related to wheat, barley, oats, and rice. *Setaria viridis,* is a C4 model grass closely related to maize, sorghum, sugarcane, and other bioenergy grasses. Both grasses are small, transformable, rapid-cycling plants with recently sequenced genomes, making them ideal model monocots for comparative analysis with Arabidopsis (Bennetzen et al., 2012; Brutnell et al., 2010). Computational analysis of *B. distachyon* has identified putative circadian clock orthologs (Higgins et al., 2010), including *BdELF3*. However, no such comparative analysis has been done systematically in *S. viridis* to identify putative orthologs of circadian clock genes. Therefore, we generated a RNA-seq time-course dataset to analyze the circadian transcriptome of *S. viridis* after either photo- or thermo-entrainment and developed an online gene-expression query tool (Diel Explorer) for the community. We found that the magnitude of circadian regulated genes in *S. viridis* is similar to other monocots after photo-entrainment, but much less after thermal entrainment. We further analyzed the functional conservation of SvELF3, together with previously reported BdELF3, by introducing both ELF3 orthologs into *A. thaliana elf3* mutant for physiological and biochemical characterization. We found that *B. distachyon* and *S. viridis* ELF3 can complement the hypocotyl elongation, flowering time and circadian arrhythmia phenotypes caused by the *elf3* mutation in *A. thaliana*. Furthermore, AP-MS analyses found that *B. distachyon* and *S. viridis* ELF3 were integrated into a similar protein-protein interaction network *in vivo* as their *A. thaliana* counterpart. Our data collectively demonstrated the functional conservation of ELF3 among *A.*

thaliana, B. distachyon and *S. Viridis* is likely due to the association with same protein partners, providing insights of how ELF3 orthologs potentially function in grasses.

RESULTS

Identifying and cloning ELF3 orthologs from *B. distachyon* and *S. viridis*

ELF3 is a plant-specific nuclear protein with conserved roles in flowering and the circadian clock in multiple plant species (Faure et al., 2012; Herrero et al., 2012; Liu et al., 2001; Lu et al., 2017; Matsubara et al., 2012; Saito et al., 2012; Weller et al., 2012; Zakhrabekova et al., 2012). To identify ELF3 orthologs in monocots, we used the protein sequence of *Arabidopsis thaliana* ELF3 (AtELF3) to search the proteomes of two model monocots *Brachypodium distachyon* and *Setaria viridis* using BLAST (Altschul et al., 1990). Among the top hits, we identified a previously reported ELF3 homolog in *B. distachyon* (*Bradi2g14290.1*, *BdELF3*) (Calixto et al., 2015; Higgins et al., 2010) and two putative *ELF3* homologous genes *Sevir.5G206400.1* (referred as *SvELF3a*) and *Sevir.3G123200.1* (referred as *SvELF3b*) in *S. viridis.* We used Clustal Omega (http://www.ebi.ac.uk/Tools/msa/clustalo/) to conduct multiple sequence alignments of comparing protein sequences of ELF3 orthologs with that of AtELF3 (Sievers et al., 2011). *BdELF3*, *SvELF3a* and *SvELF3b* encode proteins with similar identity compared to AtELF3 (34.7–36.8%) (**Supplemental Figure S1**). When compared to BdELF3, SvELF3b was 74.3% identical while SvELF3a was 57.4% identical (**Supplemental Figure S1**). Therefore, to maximize the diversity of ELF3 sequences used in this study, we cloned full length cDNAs encoding BdELF3 and SvELF3a.

Diel Explorer of *S. viridis* circadian data

In Arabidopsis, ELF3 cycles under diel and circadian conditions (constant condition after entrainment) with a peak phase in the evening (Covington et al., 2001; Hicks et al., 2001; Nusinow et al., 2011). We queried an available diurnal time course expression dataset for *B. distachyon* from the DIURNAL website, and found that *BdELF3* expression cycles under diel

conditions (LDHH, 12 h light / 12 h dark cycles with constant temperature), but not under circadian conditions in available data (LDHC-F or LDHH-F, **Supplemental Figure S2**) (Filichkin et al., 2011; Mockler et al., 2007). Also different from *AtELF3*, transcript levels of *BdELF3* accumulate at dawn rather than peak in the evening (**Supplemental Figure S2**) when grown under diel conditions, suggesting different regulations on *ELF3* expression between monocot and dicot plants. Neither diel nor circadian expression data for *S. viridis* was available. Therefore, we generated RNA-seq time-course data to examine *SvELF3* expression as well as the circadian expression of other clock orthologs after both photocycle and thermocycle entrainment. In addition, we developed the Diel Explorer tool (http://shiny.bioinformatics.danforthcenter.org/diel-explorer/) to query and visualize *S. viridis* circadian-regulated gene expression (**Supplemental Figure S3**). 48,594 *S. viridis* transcripts are represented in the two datasets entrained under either photocycles (LDHH-F) or thermocycles (LLHC-F). With Diel Explorer users can manually enter a list of transcript identifiers, gene ontology (GO) terms, or gene orthologs, plot gene expression, and download data. Alternatively, users can upload files of transcript identifiers or gene orthologs, and/or filter the datasets by entrainment, phase, or significance cut-offs. Data and graphs can be downloaded directly using Diel Explorer. The tool serves as a community resource that can be expanded to include other circadian or diurnal data in the future. The underlying code is available on Github (https://github.com/danforthcenter/diel-explorer).

Under photoperiod entrainment (LDHH-F), 5,585 of the 48,594 *S. viridis* transcripts are circadian regulated (Bonferroni-adjusted P-Value < 0.001). This proportion of photoperiod-entrained circadian genes (~11.5%) is similar to maize (10.8%), rice (12.6%), and poplar (11.2%) data sets, but much smaller than the approximately 30% reported for *A. thaliana* (Covington et al., 2008; Filichkin et al., 2011; Khan et al., 2010). Under thermocycle entrainment (LLHC-F), 582 of the 48,594 *S. viridis* transcripts are circadian regulated. Therefore, only ~1.2% of *S. viridis* transcripts are circadian cycling under thermocycle entrainment. The ~10-fold reduction in circadian cycling genes between photocycle and thermocycle entrainment (**Supplemental Figure S4**) is interesting considering that there was less than 1% difference in the number of genes with a circadian period between photocycle and

thermocycle entrainment in C3 monocot rice (*Oryza japonica*) (Filichkin et al., 2011). The reduction in cycling genes between the two entrainment conditions in *S. viridis* compared to *O. japonica* is an indication that circadian regulation could vary greatly among monocots. Also, the difference in number of cycling genes between monocots and dicots may represent a significant reduction of the role of the circadian clock between these lineages.

In addition to the overall reduction in circadian genes, the phase with the most number of cycling genes was ZT18 after light entrainment (LDHH-F; **Supplemental Figure S4**), but ZT12 with temperature entrainment (LLHC-F; **Supplemental Figure S4**), which is consistent with previous studies that have found significant differences in temperature and light entrainment of the circadian clock (Boikoglou et al., 2011; Michael et al., 2008; Michael et al., 2003). There are 269 genes that are considered circadian-regulated and are cycling under both LDHH-F and LLHC-F conditions (Bonferroni Adjusted P-Value < 0.001). The list of 269 genes that overlap between photocycle and thermocycle entrainment includes best matches for Arabidopsis core clock components *TIMING OF CAB EXPRESSION 1* (*TOC1, AT5G61380.1*; *Sevir.1G241000.1*), *LATE ELONGATED HYPOCOTYL* (*LHY, AT1G01060*; *Sevir.6G053100.1*), and *CCA1*-like gene *REVEILLE1* (*RVE1*, *AT5G17300.1*; *Sevir.1G280700.1*). However, putative *S. viridis* orthologs of *TOC1*, *LHY*, and *RVE1* all have different circadian phases under LDHH entrainment compared to LLHC entrainment (**Figure 1**). In fact, the majority (233/269) of overlapping circadian genes in *S. viridis* have a distinct circadian phase under thermocyle compared to photocyle entrainment (**Supplemental Figure S4**). We also found that putative orthologs of *PSEUDO-RESPONSE REGULATOR 7* (*PRR7*, *AT5G02810*; *Sevir.2G456400.1*; related to *OsPRR73* (Murakami et al., 2003)) and *LUX ARRHYTHMO* (*LUX*, *AT3G46640*; *Sevir.5G474200.1*) cycle significantly under LDHH-F but not LLHC-F conditions (**Figure 1**). Neither *SvELF3a* nor *SvELF3b* cycle under circadian conditions after photo- or thermo-entrainment (**Figure 1**), similar to ELF3 orthologs in *B. distachyon* (**Supplemental Figure S2**) (Mockler et al., 2007) and *O. sativa* (Filichkin et al., 2011). This is different from *AtELF3*, which continues to cycle under constant condition after either photo- or thermos-entrainment (**Supplemental Figure S5**) (Mockler et al., 2007). The difference in expression of these putative orthologs between *A. thaliana* and

monocots *S. viridis*, *B. distachyon*, and *O. sativa*, suggest that the architecture of the circadian clock may have significant differences in response to environmental cues in these two species.

BdELF3 and SvELF3 rescue growth and flowering defects in *Arabidopsis elf3* mutant

Although the circadian expression pattern of *B. distachyon ELF3* and *S. viridis ELF3* is different from that of *A. thaliana ELF3*, it is still possible that the ELF3 orthologs have conserved biological functions. To test this, we sought to determine if BdELF3 or SvELF3a could complement the major phenotypic defects of the *elf3* mutant in *A. thaliana*, namely hypocotyl elongation, time to flowering, or circadian rhythmicity. To this end, we constitutively expressed *BdELF3*, *SvELF3a* (hereafter referred as *SvELF3*) and *AtELF3* cDNAs by the *35S Cauliflower mosaic virus* promoter in the *A. thaliana elf3-2* mutant expressing a *LUCIFERASE* reporter driven by the promoter of *CIRCADIAN CLOCK ASSOCIATED 1* (*CCA1*) (*elf3-2* [*CCA1:LUC*]) (Pruneda-Paz et al., 2009). All three ELF3 coding sequences were fused to a C-terminal His_6-3xFlag affinity tag (HFC), which enables detection by western blotting and identification of protein-protein interaction by affinity purification and mass spectrometry (AP-MS) (Huang et al., 2016a). After transforming these constructs, we identified and selected two biologically independent transgenic lines with a single insertion of each At/Bd/SvELF3-HFC construct. Western blot analysis using FLAG antibodies detected the expression of all ELF3-HFC fusion proteins (**Supplemental Figure S6**).

Next, we asked if expressing At/Bd/SvELF3-HFC fusion proteins could rescue the mutation defects caused by *elf3-2*. When plants are grown under light/dark cycles (12 hour light: 12 hour dark), *elf3-2* mutant plants elongate their hypocotyls much more than wild type plants (4.75±0.48 mm vs. 1.95±0.27 mm, respectively. ± = standard deviation) (**Figure 2**). The long hypocotyl defect in *elf3-2* was effectively suppressed by expressing either *AtELF3*, or *ELF3* orthologs (*BdELF3 or SvELF3a*) (**Figure 2**). These data show that the monocot *ELF3* orthologs function similarly to *A. thaliana ELF3* in the regulation of hypocotyl elongation in seedlings.

In addition to regulating phenotypes in seedlings, ELF3 also functions in adult plants to suppress the floral transition. Loss-of-function in Arabidopsis *ELF3* results in an early flowering phenotype regardless of day-length (Hicks et al., 2001; Liu et al., 2001; Zagotta et al., 1992). To determine how monocot ELF3 orthologs compared to *A. thaliana* ELF3 in flowering time regulation, we compared flowering responses under long day conditions among wild type, *elf3-2*, and *elf3-2* transgenic lines expressing *AtELF3*, *BdELF3*, or *SvELF3* (At/Bd/SvELF3-HFC). Constitutive over-expression of *AtELF3* led to a delay in flowering in long days (**Figure 3**) as previously observed (Liu et al., 2001). Similarly, constitutive expression of *BdELF3* or *SvELF3* caused plants to flower significantly later than the *elf3* mutants. These data show that all *ELF3* orthologs can function to repress the rapid transition to flowering of the *elf3* mutation when constitutively expressed in adult plants.

BdELF3 and SvELF3 restore the circadian rhythmicity in *Arabidopsis elf3* mutant

ELF3 is a key component of the *A. thaliana* circadian clock and is critical for maintaining the periodicity and amplitude of rhythms as shown using the *CCA1* promoter driven luciferase reporter (CCA:LUC) (Covington et al., 2001; Hicks et al., 1996; Nusinow et al., 2011). To determine if *BdELF3* or *SvELF3*a could rescue the arrhythmic phenotype of the *elf3* mutation, we analyzed the rhythms of the *CCA1::LUC* reporter under constant light conditions after diel entrainment (12 hours light: 12 hours dark at constant 22 ˚C). Relative amplitude error (RAE) analysis found that 100% of wild type and all three *elf3-2* transgenic lines expressing *AtELF3*, *BdELF3*, and *SvELF3* were rhythmic, while only 50% of the *elf3-2* lines had rhythms (RAE < 0.5) (**Supplemental Figure S7**). Comparison of average period length found that the *AtELF3* and *SvELF3* expressing lines rescued the period and amplitude defects in the *elf3* mutant (**Figure 4A**, **4C** and **4D**). While the *BdELF3* lines rescued the amplitude defect (**Figure 4B**), their period was significantly divergent from wild type (compare 23.21 ± 0.59 hours for wild type to *BdELF3 #2*= 26.03 ± 1.33 hours, *BdELF3 #3*= 26.86 ± 0.81 hours, *elf3-2*= 26.54 ± 5.02 hours, ± = standard deviation, **Figure 4D**). In summary, these data show that expression of any of the ELF3 orthologs is sufficient to recover the amplitude and restore circadian rhythms of the *CCA1::LUC* reporter.

306

307 **BdELF3 and SvELF3 are integrated into a similar protein-protein interaction network in**
308 ***A. thaliana***

309

310 Despite relatively low sequence conservation at the protein level, the *ELF3* orthologs can
311 complement a wide array of *elf3* phenotypes (**Figures 2** to **4**). As ELF3 functions within the
312 evening complex (EC) in Arabidopsis, which also contains the transcription factor LUX and the
313 DUF-1313 domain containing protein ELF4 (Herrero et al., 2012; Nusinow et al., 2011), we
314 reasoned that the monocot *ELF3* orthologs may also be able to bind to these proteins when
315 expressed in *A. thaliana*. To determine if a composite EC could be formed, we tested if BdELF3
316 or SvELF3a could directly interact with AtLUX or AtELF4 in a yeast two-hybrid assay. Similar
317 to AtELF3 (Nusinow et al., 2011), both BdELF3 and SvELF3a directly interact with both
318 AtELF4 and the C-terminal portion of AtLUX (**Figure 5**). We cannot conclude that whether
319 monocot ELF3 orthologs are also able to interact with the N-terminal AtLUX, since this
320 fragment auto-activated the reporter gene in the yeast two-hybrid assay (**Figure 5**).

321

322 ELF3 functions not only as the scaffold of the EC, but also as a hub protein in a protein-protein
323 interaction network containing multiple key regulators in both the circadian clock and light
324 signaling pathways (Huang et al., 2016a; Huang and Nusinow, 2016b). We hypothesize that
325 BdELF3 and SvELF3 could rescue many of the defects of the *elf3* mutant because both monocot
326 versions were integrated into the same protein-protein interaction network. To test this
327 hypothesis, we used affinity purification and mass spectrometry (AP-MS) to identify the proteins
328 that co-precipitate with monocot ELF3s when expressed in *A. thaliana*. AP-MS on two
329 biological replicates for each sample with the above-mentioned independent insertion lines were
330 included for each ELF3 ortholog. For comparison, the same AP-MS experiment was done with
331 one of the 35S promoter-driven AtELF3-HFC transgenic lines (AtELF3-2). To detect specific
332 co-precipitating proteins, we manually removed commonly identified contaminant proteins from
333 plant affinity purifications and mass spectrometry experiments (Van Leene et al., 2015), and
334 proteins identified from a control transgenic line expressing GFP-His_6-3xFlag described

335 previously (Huang et al., 2016a) (**Table 1**, the full list of identified proteins can be found in
336 **Supplemental Table S2**).
337
338 We have previously reported proteins that co-precipitated with ELF3 driven from its native
339 promoter using a similar AP-MS methodology (Huang et al., 2016a). When using the 35S
340 promoter driven AtELF3 transgenic line, we were able to generate a curated list of 22 proteins
341 that specifically co-precipitate with AtELF3, including all previously identified proteins, such as
342 all five phytochromes, PHOTOPERIODIC CONTROL OF HYPOCOTYL1 (PCH1) (Huang et
343 al., 2016c), and COP1 (**Table 1**). In addition, we also identified LIGHT-REGULATED WD 2
344 (LWD2) and SPA1-RELATED 4 (SPA4) as now co-precipitating with AtELF3. These additional
345 interactions may be a result of a combination of altered seedling age, expression level of the
346 ELF3 bait, or tissue-specificity of expression due to these purifications are from tissues where
347 the epitope-tagged transgene is constitutively over-expressed. However, since LWD2 is a known
348 component of the circadian clock (Wu et al., 2008) and SPA4 is a known component of the
349 COP1-SPA complex (Zhu et al., 2008), these interactions are likely to be relevant.
350
351 In comparing the list of BdELF3 and SvELF3 co-precipitated proteins with that of AtELF3, we
352 found that neither SvELF3 nor BdELF3 co-precipitated SPA2 and SPA4, components of the
353 COP1-SPA complex. In addition, SvELF3 did not co-precipitate MUT9-LIKE KINASE1, a
354 kinase with roles in chromatin modification and circadian rhythms as AtELF3 did (Huang et al.,
355 2016a; Wang et al., 2015). However, BdELF3 and SvELF3 associated with most of the proteins
356 found in AtELF3 AP-MS (20 out of 22 for BdELF3, 19 out of 22 for SvELF3), in at least one of
357 the replicate purifications from each monocot ortholog AP-MS. Therefore our data suggest that
358 BdELF3 and SvELF3 are integrated into a similar protein-protein interaction network as
359 AtELF3, which likely underlies their ability of broadly complementing *elf3* mutants.
360
361 **DISCUSSION**
362
363 Recent work in diverse plant species has found that the circadian clock plays critical roles in
364 regulating metabolism, growth, photoperiodism, and other agriculturally important traits (Bendix

et al., 2015; McClung, 2013; Shor and Green, 2016). While the relevance of the circadian clock to plant fitness is unquestioned, it is unclear if the circadian clock components have conserved function among different plant species. This is particularly true for the majority of clock proteins, whose biological functions are currently poorly understood at the molecular level (Hsu and Harmer, 2014). Also, the divergent modes of growth regulation and photoperiodism between monocots and dicots suggest that the clock evolved to have altered roles in regulating these physiological responses between lineages (Matos et al., 2014; Poire et al., 2010; Song et al., 2014). Here we asked if orthologs of ELF3 from two monocots could complement any of the loss-of-function phenotypes in the model dicot plant *A. thaliana*. In this study we found that ELF3 from either *B. distachyon* or *S. viridis* could complement the hypocotyl elongation, early flowering, and arrhythmic clock phenotype of the *elf3* mutant in *A. thaliana*, despite the variations in protein sequences and evolutionary divergence between monocot and dicot plants. These data suggest that monocot ELF3s can functionally substitute for *A. thaliana* ELF3, albeit with varying efficacy. Since monocot and dicot ELF3 are largely different in the protein sequences, functional conservation of ELF3 orthologs also leads to the next open question of identifying the functional domains within ELF3.

Previously, comparison of ELF3 homologs has identified at least five conserved regions that may be important for function (**Supplemental Figure S1**) (Liu et al., 2001; Saito et al., 2012; Weller et al., 2012). Our multiple sequence alignments also show that at least two regions of AtELF3, namely the N-terminus (AA 1~49) and one middle region (AA 317~389) share many conserved residues with ELF3 orthologs in grasses (**Supplemental Figure S1**). These regions fall within known fragments that are sufficient for binding to phyB (Liu et al., 2001), COP1 (Yu et al., 2008), or ELF4 (Herrero et al., 2012). Consistent with the hypothesis that these conserved regions are critical for proper ELF3 function, a single amino acid substitution (A362V) within this middle region results in defects of ELF3 nuclear localization and changes in the circadian clock period (Anwer et al., 2014). In addition, our protein-protein interaction study and AP-MS analysis show that both monocot ELF3 can form composite ECs (**Figure 5**) and that all three ELF3 homologs interact with an almost identical set of proteins *in vivo* (**Table 1**), further suggesting that one or more of the conserved regions may mediate the binding between ELF3

and its known interacting proteins. Furthermore, the similar pool of ELF3 interacting proteins identified by Bd/SvELF3 AP-MS suggests that the overall conformation of ELF3 ortholog proteins is conserved and that similar complexes and interactions with ELF3 orthologs may form in monocot species. However, whether these interactions form *in planta* and have the same effect on physiology is unclear. For example, *S. viridis* data generated here and public data for *B. distachyon* and *O. sativa*, showed that ELF3 does not cycle under circadian conditions, which differs from Arabidopsis. Further, different from the fact that the clock plays a key role in regulating elongation in *A. thaliana* (Nozue et al., 2007), the circadian clock has no influence on growth in C3 model grass *B. distachyon*, despite robust oscillating expression of putative clock components (Matos et al., 2014). Similarly, ELF3 from rice *(Oryza sativa)* and soybean promotes flowering and senescence (Lu et al., 2017; Saito et al., 2012; Sakuraba et al., 2016; Yang et al., 2013; Zhao et al., 2012), while in *A. thaliana*, ELF3 represses these responses (Liu et al., 2001; Sakuraba et al., 2014; Zagotta et al., 1992), which suggests significant rewiring of ELF3 regulated photoperiodic responses of flowering between short-day (rice/soybean) and long-day (*A. thaliana*) plants. Alternatively, ELF3 may form distinct interactions and complexes in monocot species that were not identified in our trans-species complementation analysis. Clearly, further work is required to understand ELF3 function in monocots beyond the studies presented here.

In addition to the molecular characterization of ELF3, our analysis of circadian-regulated genes in *S. viridis* after photo- and thermo-entrainment found significant differences in the behavior of the clock when compared to other monocots. Although the number of circadian regulated genes is comparable to studies done in corn and rice after photo-entrainment (between 10-12%) (Filichkin et al., 2011; Khan et al., 2010), we found that very few genes (~1%) continue to cycle after release from temperature entrainment in *S. viridis* (**Supplemental Figure S4**) when compared to rice (~11%) (Filichkin et al., 2011). This may reflect a fundamental difference in how the clock interfaces with temperature between these monocot species. Furthermore, proportions of circadian regulated genes upon photo-entrainment in all three monocot plants (**Supplement Figure S4**) (Filichkin et al., 2011; Khan et al., 2010) are much smaller than the approximately 30% reported for *A. thaliana* (Covington et al., 2008), suggesting the divergence

of clock functions through evolution or domestication. Further comparisons of circadian responses among monocots or between monocots and dicots will help to determine the molecular underpinning of these differences.

In summary, we find that BdELF3 and SvELF3 form similar protein complexes *in vivo* as AtELF3, which likely allows for functional complementation of loss-of-function of *elf3* despite relatively low sequence conservation. We also present an online query tool, Diel Explorer that allows for exploration of circadian gene expression in *S. viridis*, which illustrate fundamental differences in clock function among monocots and between monocots and dicots. Collectively, this work is a first step toward functional understanding of the circadian clock in two model monocots, *S. viridis* and *B. distachyon.*

MATERIALS AND METHODS

Plant materials and growth conditions

For *A. thaliana*, wild type (Columbia-0) and *elf3-2* plants carrying the CCA1::LUC reporter were described previously (Nusinow et al., 2011; Pruneda-Paz et al., 2009). Seeds were surface sterilized and plated on 1/2x Murashige and Skoog (MS) basal salt medium with 0.8% agar + 1% (w/v) sucrose. After 3 days of stratification, plates were placed horizontally in a Percival incubator (Percival Scientific, Perry, IA), supplied with 80 µmol m^{-2} sec^{-1} white light and set to a constant temperature of 22°C. Plants were grown under 12 h light / 12 h dark cycles (12L:12D) for 4 days (for physiological experiments) or for 10 days (for AP-MS) before assays.

For *S. viridis* circadian expression profiling by RNA-seq, seeds were stratified for 5 days at 4°C before being moved to entrainment conditions. Plants were grown under either LDHH or LLHC (L: light, D: dark, H: hot, C: cold) entrainment condition, and then sampled for RNA-seq in constant light and constant temperature (32°C) conditions (F, for free-running) every 2 hours for 48 hours. Light intensity was set to 400 µmol m^{-2} sec^{-1} white light. In LDHH-F, stratified *S. viridis* seeds were grown for 10 days under 12L:12D and constant temperature (32°C) before

455 sampling in constant light and constant temperature. In LLHC-F, stratified *S. viridis* seeds were
456 grown for 10 days under constant light conditions and cycling temperature conditions 12 h at
457 32°C (subjective day) / 12 h at 22°C (subjective night) before sampling in constant conditions.
458 Two experimental replicates were collected for each entrainment condition.
459
460 **Setaria circadian RNA-seq**
461
462 The second leaf from the top of seventeen *S. viridis* plants was selected for RNA-seq sampling at
463 each time point for each sampling condition. Five replicate samples were pooled after being
464 ground in liquid nitrogen and resuspended in lithium chloride lysis binding buffer (Wang et al.,
465 2011a). RNA-seq libraries from leaf samples were constructed according to the previous
466 literature (Wang et al., 2011a) with one major modification. Rather than extracting RNA then
467 mRNA from ground leaf samples (Wang et al., 2011a), mRNA was extracted directly from
468 frozen ground leaf samples similar to the method described in (Kumar et al., 2012), except that
469 two additional rounds of wash, binding, and elution steps after treatment with EDTA were
470 necessary to remove rRNA from samples. mRNA quantity was assessed using a Qubit with a
471 Qubit RNA HS Kit and mRNA quality was assessed using a Bioanalyzer and Plant RNA PiCO
472 chip. 96 library samples were multiplexed 12 per lane, for a total of 8 lanes of Illumina Hiseq
473 2000 sequencing. Paired end 101 bp Sequencing was done at MOgene (St. Louis, MO). Raw
474 data and processed data can be found on NCBI's Gene Expression Omnibus (GEO; (Barrett et
475 al., 2013; Edgar et al., 2002)) and are accessible with identification number GSE97739
476 (https://www.ncbi.nlm.nih.gov/geo/query/acc.cgi?acc=GSE97739).
477
478 RNA-seq data was trimmed with BBTools (v36.20) using parameters: ktrim=r k=23 mink=11
479 hdist=1 tpe tbo ktrim=l k=23 mink=11 hdist=1 tpe tbo qtrim=rl trimq=20 minlen=20 (Bushnell,
480 2016). Any parameters not specified were run as default. Before trimming we had 1,814,939,650
481 reads with a mean of 18,905,621 reads per sample and a standard deviation of 2,875,187. After
482 trimming, we have 1,646,019,593 reads with a mean of 17,146,037 reads per sample and a
483 standard deviation of 2,411,061. Kallisto (v 0.42.4; (Bray et al., 2016)) was used to index the
484 transcripts with the default parameters and the *S. viridis* transcripts fasta file (Sviridis_311_v1.1)

from Phytozome (Goodstein et al., 2012). The reads were quantified with parameters:-t 40 -b 100. Any parameters not specified were run as default. Kallisto output was formatted for compatibility with JTKCycle (v3.1; (Hughes et al., 2010)) and circadian cycles were detected. To query the *S. viridis* expression data we developed Diel Explorer. The tool can be found at http://shiny.bioinformatics.danforthcenter.org/diel-explorer/. Underlying code for Diel Explorer is available on Github (https://github.com/danforthcenter/diel-explorer).

Plasmid constructs and generation of transgenic plants

Coding sequences (without the stop codon) of *AtELF3* (*AT2G25930*) and *SvELF3a* (*Sevir.5G206400.1*) were cloned into the pENTR/D-TOPO vector (ThermoFisher Scientific, Waltham, MA), verified by sequencing and were recombined into the pB7HFC vector (Huang et al., 2016a) using LR Clonease (ThermoFisher Scientific, Waltham, MA). Coding sequence of BdELF3 (*Bradi2g14290.1*) was submitted to the U.S. Department of Energy Joint Genome Institute (DOE-JGI), synthesized by the DNA Synthesis Science group, and cloned into the pENTR/D-TOPO vector. Sequence validated clones were then recombined into pB7HFC as described above. The pB7HFC-At/Bd/SvELF3 constructs were then transformed into *elf3-2* [*CCA1::LUC*] plants by the floral dip method (Zhang et al., 2006). Homozygous transgenic plants were validated by testing luciferase bioluminescence, drug resistance, and by PCR-based genotyping. All primers used in this paper were listed in **Supplemental Table S1**.

Hypocotyl and flowering time measurement

20 seedlings of each genotype were arrayed and photographed with a ruler for measuring hypocotyl length using the ImageJ software (NIH) (Schneider et al., 2012). The procedure was repeated three times. For measuring flowering time, 12 plants of each genotype were placed in a random order and were grown under the long day condition (light : dark = 16 : 8 hours). The seedlings were then observed every day at 12:00 PM; the date on which each seedling began flowering, indicated by the growth of a ~1 cm inflorescence stem, was recorded along with the number of rosette leaves produced up to that date.

515

516 **Circadian assays in *A. thaliana***

517

518 Seedlings were transferred to fresh 1/2x MS plates after 5 days of entrainment under the
519 12L:12D condition and sprayed with sterile 5 mM luciferin (Gold Biotechnology, St. Louis, MO)
520 prepared in 0.1% (v/v) Triton X-100 solution. Sprayed seedlings were then imaged in constant
521 light (70 µmol m^{-2} sec^{-1}, wavelengths 400, 430, 450, 530, 630, and 660 set at intensity 350
522 (Heliospectra LED lights, Göteborg, Sweden)). Bioluminescence was recorded after a 120-180s
523 delay to diminish delayed fluorescence (Gould et al., 2009) over 5 days using an ultra-cooled
524 CCD camera (Pixis 1024B, Princeton Instruments) driven by Micro-Manager software (Edelstein
525 et al., 2010; Edelstein et al., 2014). The images were processed in stacks by Metamorph software
526 (Molecular Devices, Sunnyvale, CA), and rhythms determined by fast Fourier transformed non-
527 linear least squares (FFT-NLLS) (Plautz et al., 1997) using the interface provided by the
528 Biological Rhythms Analysis Software System 3.0 (BRASS) available at http://www.amillar.org.

529

530 **Yeast two-hybrid analysis**

531

532 Yeast two-hybrid assays were carried out as previously described (Huang et al., 2016a). In brief,
533 the DNA binding domain (DBD) or activating domain (AD)-fused constructs were transformed
534 using the Li-Ac transformation protocol (Clontech) into *Saccharomyces cerevisiae* strain Y187
535 (MATα) and the AH109 (MATa), respectively. Two strains of yeast were then mated to generate
536 diploid with both DBD and AD constructs. Protein-protein interaction was tested in diploid yeast
537 by replica plating on CSM –Leu –Trp –His media supplemented with extra Adenine (30mg/L
538 final concentration) and 2mM 3-Amino-1,2,4-triazole (3AT). Pictures were taken after 4-day
539 incubation at 30 ˚C. All primers used for cloning plasmid constructs were listed in
540 **Supplemental Table S1**.

541

542 **Protein extraction and western blotting**

543

Protein extracts were made from 10-day-old seedlings as previously described (Huang et al., 2016a) and loaded 50 µg to run 10% SDS-PAGE. For western blots, all of the following primary and secondary antibodies were diluted into PBS + 0.1% Tween and incubated at room temperature for 1 hour: anti-FLAG®M2-HRP (Sigma, A8592, diluted at 1:10,000) and anti-Rpt5-rabbit (ENZO Life Science, BML-PW8245-0025, diluted at 1:5000) and anti-Rabbit-HRP secondary antibodies (Sigma, A0545, diluted at 1:10,000).

Affinity purification and mass spectrometry

Protein extraction methods and protocols for AP-MS were described previously (Huang et al., 2016a; Huang et al., 2016b; Huang and Nusinow, 2016a; Huang et al., 2016c)}. In brief, transgenic seedlings carrying the At/Bd/SvELF3-HFC constructs were grown under 12L:12D conditions for 10 days and were harvested at dusk (ZT12). 5 grams of seedlings were needed per replicate to make protein extracts, which underwent tandem affinity purification utilizing the FLAG and His epitopes of the fusion protein. Purified samples were reduced, alkylated and digested by trypsin. The tryptic peptides were then injected to an LTQ-Orbitrap Velos Pro (ThermoFisher Scientific, Waltham, MA) coupled with a U3000 RSLCnano HPLC (ThermoFisher Scientific, Waltham, MA) with settings described previously (Huang et al., 2016a).

AP-MS data analysis

Data analysis was done as previously described (Huang et al., 2016a). The databases searched were TAIR10 database (20101214, 35,386 entries) and the cRAP database (http://www.thegpm.org/cRAP/). Peptide identifications were accepted if they could be established at greater than 95.0% probability and the Scaffold Local FDR was <1%. Protein identifications were accepted if they could be established at greater than 99.0% probability as assigned by the Protein Prophet algorithm (Keller et al., 2002; Nesvizhskii et al., 2003). A full list of all identified proteins (reporting total/exclusive unique peptide count and percent coverage) can be found in **Supplemental Table S2**. The mass spectrometry proteomics data

574 have been deposited to the ProteomeXchange Consortium (Vizcaino et al., 2014) via the PRIDE
575 partner repository with the dataset identifier PXD006352 and 10.6019/PXD006352.
576
577
578 **Supplemental Data**
579 **Supplemental Table S1.** List of all primers used.
580 **Supplemental Table S2.** A full list of At/Bd/SvELF3 associated proteins identified from AP-
581 MS.
582 **Supplemental Figure S1.** Multiple sequence alignments of ELF3 orthologs **Supplemental**
583 **Figure S2.** Diel and circadian expression of *BdELF3* from the DIURNAL database.
584 **Supplemental Figure S3.** Example of the Diel Explorer interface.
585 **Supplemental Figure S4.** Summary of circadian regulated genes in *S. viridis.*
586 **Supplemental Figure S5.** Circadian expression of selected *A. thaliana* clock genes from the
587 DIURNAL database.
588 **Supplemental Figure S6.** Anti-FLAG western of ELF3 transgenic lines used for
589 complementation analysis.
590 **Supplemental Figure S7.** Relative Amplitude Error vs period plots of transgenic *elf3-2* plants
591 expressing At/Bd/SvELF3.
592

Table 1. Proteins co-purified with ELF3 orthologs from AP-MS

AGI number	Protein Name	Molecular Weight	Exclusive Unique Peptide Count/Percent Coverage[a]									
			AtELF3		SvELF3 #2		SvELF3 #3		BdELF3 #2		BdELF3 #3	
			rep1	rep2	rep1	rep2	rep1	rep2	rep1	rep2	rep1	rep2
n/a	AtELF3-HFC	84 kDa	20/36%	19/31%	—	—	—	—	—	—	—	—
n/a	SvELF3-HFC	87 kDa	—	—	19/40%	29/48%	22/42%	33/54%	—	—	—	—
n/a	BdELF3-HFC	86 kDa	—	—	—	—	—	—	25/42%	26/43%	21/35%	19/33%
AT2G18790	phyB	129 kDa	23/37%	24/37%	31/54%	28/42%	32/50%	30/45%	22/34%	22/33%	24/40%	24/37%
AT5G35840	phyC	124 kDa	22/29%	23/29%	27/37%	32/39%	27/37%	33/42%	20/24%	18/22%	19/23%	22/27%
AT5G43630	TZP	91 kDa	14/21%	12/17%	13/23%	20/33%	13/22%	24/36%	12/18%	13/19%	14/20%	14/22%
AT4G18130	phyE	123 kDa	11/16%	19/27%	12/18%	18/23%	11/19%	17/24%	6/7%	10/14%	14/19%	13/18%
AT2G16365.2	PCH1b	51 kDa	9/25%	9/25%	9/30%	14/43%	11/36%	16/49%	9/26%	9/28%	11/32%	11/32%
AT2G46340	SPA1	115 kDa	8/14%	7/9%	2/2%	4/8%	2/3%	4/9%	—	—	6/8%	5/6%
AT3G42170c	DAYSLEEPER	79 kDa	8/19%	5/11%	—	7/16%	—	12/27%	3/7%	4/8%	2/4%	—
AT2G32950	COP1	76 kDa	8/16%	9/17%	6/17%	4/8%	3/6%	5/12%	1/2%	2/4%	6/11%	4/8%
AT3G22380	TIC	165 kDa	5/5%	5/5%	4/4%	12/12%	3/3%	15/15%	4/4%	3/3%	1/1%	1/1%
AT4G11110	SPA2	115 kDa	5/11%	6/12%	—	—	—	—	—	—	—	—
AT2G40080	ELF4	12 kDa	4/50%	4/50%	3/42%	5/68%	4/60%	4/60%	4/50%	4/50%	5/68%	5/68%
AT1G09340c	CRB	43 kDa	4/16%	3/12%	1/4%	1/4%	1/4%	4/18%	1/4%	1/4%	—	—
AT3G13670	MLK4	79 kDa	3/10%	3/13%	—	—	—	1/2%	6/21%	3/10%	3/11%	5/13%
AT5G61380	TOC1	69 kDa	2/4%	2/4%	2/5%	—	3/7%	—	—	—	1/2%	1/2%
AT1G53090	SPA4	89 kDa	2/6%	5/14%	—	—	—	—	—	—	—	—
AT5G18190	MLK1	77 kDa	2/12%	2/11%	—	—	—	—	2/14%	2/14%	2/11%	2/11%
AT3G26640	LWD2	39 kDa	2/21%	1/21%	—	1/16%	—	2/22%	3/27%	1/16%	—	—
AT1G12910	LWD1	39 kDa	2/21%	3/30%	2/21%	4/31%	1/17%	2/21%	2/22%	2/19%	0/11%	0/11%
AT4G16250	phyD	129 kDa	1/10%	1/11%	2/12%	1/12%	3/15%	2/12%	2/11%	1/10%	2/14%	2/12%
AT1G09570	phyA	125 kDa	1/1%	1/1%	7/11%	5/5%	7/11%	2/2%	—	2/2%	6/7%	3/4%

AT2G25760	MLK3	76 kDa	1/5%	1/6%	—	1/4%	—	1/4%	3/13%	2/9%	2/9%	2/9%
AT3G03940	MLK2	78 kDa	1/8%	1/8%	—	1/7%	—	0/2%	3/20%	2/13%	3/13%	1/9%
AT3G46640	LUX	35 kDa	1/3%	1/3%	0/10%	3/19%	0/10%	3/23%	1/3%	1/3%	1/3%	2/11%
AT1G17455	ELF4-L4	13 kDa	—	—	—	—	—	—	1/23%	1/23%	—	—
AT1G72630	ELF4-L2	13 kDa	—	1/11%	—	1/13%	—	—	1/22%	1/22%	1/22%	1/11%

Proteins co-purified with ELF3 orthologs (AtELF3, SvELF3 and BdELF3, with C-terminal His6-3xFLAG tag) were identified from affinity purification coupled with mass spectrometry (AP-MS) analyses using 12L:12D grown, 10-day-old transgenic plants (in *elf3-2 null* mutant backgrounds) harvested at ZT12.

[a] All listed proteins match 99% protein threshold, minimum number peptides of 2 and peptide threshold as 95%. Proteins not matching the criteria were marked with "—".

[b] Percent coverage for PCH1 is calculated using protein encoded by *At2g16365.2*

[c] These proteins have been noted as frequently identified proteins in AP-MS experiments (see Van Leene, 2015).

FIGURE LEGENDS

Figure 1. Circadian expression profiles of putative *S. viridis* clock components from Diel Explorer using time-course RNA-seq data. *S. viridis* plants were entrained by either photocycle (LDHH) or thermocycle (LLHC), followed by being sampled every 2 hours for 48 hours under constant temperature and light conditions (Free-Running; F) to generate time-course RNA-seq data. Mean values of Transcripts per Kilobase Million (TPM) from two experimental replicates for each timepoints per gene were plotted.

Figure 2. ELF3 orthologs suppress hypocotyl elongation defects in *elf3-2*. The hypocotyls of 20 seedlings of wild type, *elf3-2* mutant, AtELF3 *elf3-2*, BdELF3 *elf3-2*, and SvELF3 *elf3-2* (two independent transgenic lines for each ELF3 ortholog) were measured at 4 days after germination under 12-hour light :12-hour dark growth conditions at 22 ˚C. Upper panel shows representative seedlings of each genotype, with scale bar equal to 5 mm. Mean and 95% confidence intervals are plotted as crosshairs. This experiment was repeated three times with similar results. ANOVA analysis with Bonferroni correction was used to generate adjusted P values, * < 0.05, ** < 0.01, **** < 0.0001**.**

Figure 3. ELF3 orthologs suppress time to flowering of *elf3-2*. 12 wild type, *elf3-2* mutant, AtELF3 *elf3-2*, BdELF3 *elf3-2*, and SvELF3 *elf3-2* seedlings from two independent transformations were measured for days **(A)** and number of rosette leaves **(B)** at flowering (1 cm inflorescence). Mean and 95% confidence intervals are plotted as crosshairs. This experiment was repeated twice with similar results. ANOVA analysis with Bonferroni correction was used to generate adjusted P values, ** < 0.01, *** < 0.001, **** < 0.0001, of measurements when compared to the *elf3-2* mutant line.

Figure 4. ELF3 orthologs can recover *CCA1::LUC* rhythms and amplitude in *elf3-2* mutants. 8 seedlings of wild type, *elf3-2* mutant, AtELF3 *elf3-2* **(A)**, BdELF3 *elf3-2* **(B)**, and SvELF3 *elf3-2* **(C)** from two independent transformations were imaged for bioluminescence under constant light after entrainment in 12-hour light :12-hour dark growth conditions at 22 ˚C. Each plot shows

623 average bioluminescence of all seedlings along with 95% confidence interval (error bars). This
624 experiment was repeated twice with similar results. Note that wild type and *elf3-2* mutant data
625 was plotted on all graphs for comparison. **(D)** Periods of seedlings. Only periods with a Relative
626 Amplitude Error below 0.5 (see **Supplemental Figure S7**) were plotted. Mean and 95%
627 confidence intervals are plotted as crosshairs. ANOVA analysis with Bonferroni correction was
628 used to generate adjusted P values, ** < 0.01, *** < 0.001, **** < 0.0001, of measurements
629 when compared to the wild type.
630
631 **Figure 5.** Both BdELF3 and SvELF3 can directly bind to AtELF4 and AtLUX. Yeast two-hybrid
632 analysis of testing if either BdELF3 **(A)** or SvELF3 **(B)** can directly interact with either AtELF4,
633 the N-terminal half of AtLUX (AtLUX-N, a.a. 1-143) or the C-terminal half of AtLUX (AtLUX-
634 C, a.a. 144-324). –LW tests for the presence of both bait (DBD) and pray (AD) vectors, while the
635 –LWH + 3AT tests for interaction. Vector alone serves as interaction control. This experiment
636 was repeated twice with similar results.
637
638
639
640 **REFERENCES**
641
642 Altschul, S.F., Gish, W., Miller, W., Myers, E.W., and Lipman, D.J. (1990). Basic local alignment
643 search tool. J Mol Biol *215*, 403-410.
644 Anwer, M.U., Boikoglou, E., Herrero, E., Hallstein, M., Davis, A.M., Velikkakam James, G., Nagy,
645 F., and Davis, S.J. (2014). Natural variation reveals that intracellular distribution of ELF3 protein
646 is associated with function in the circadian clock. Elife *3*.
647 Barrett, T., Wilhite, S.E., Ledoux, P., Evangelista, C., Kim, I.F., Tomashevsky, M., Marshall, K.A.,
648 Phillippy, K.H., Sherman, P.M., Holko, M.*, et al.* (2013). NCBI GEO: archive for functional
649 genomics data sets--update. Nucleic Acids Res *41*, D991-995.
650 Bell-Pedersen, D., Cassone, V.M., Earnest, D.J., Golden, S.S., Hardin, P.E., Thomas, T.L., and
651 Zoran, M.J. (2005). Circadian rhythms from multiple oscillators: lessons from diverse organisms.
652 Nat Rev Genet *6*, 544-556.
653 Bendix, C., Marshall, C.M., and Harmon, F.G. (2015). Circadian Clock Genes Universally Control
654 Key Agricultural Traits. Mol Plant *8*, 1135-1152.

655 Bennetzen, J.L., Schmutz, J., Wang, H., Percifield, R., Hawkins, J., Pontaroli, A.C., Estep, M., Feng,
656 L., Vaughn, J.N., Grimwood, J.*, et al.* (2012). Reference genome sequence of the model plant
657 Setaria. Nat Biotechnol *30*, 555-561.
658 Boikoglou, E., Ma, Z., von Korff, M., Davis, A.M., Nagy, F., and Davis, S.J. (2011). Environmental
659 memory from a circadian oscillator: the Arabidopsis thaliana clock differentially integrates
660 perception of photic vs. thermal entrainment. Genetics *189*, 655-664.
661 Bray, N.L., Pimentel, H., Melsted, P., and Pachter, L. (2016). Near-optimal probabilistic RNA-seq
662 quantification. Nat Biotech *34*, 525-527.
663 Brutnell, T.P., Wang, L., Swartwood, K., Goldschmidt, A., Jackson, D., Zhu, X.G., Kellogg, E., and
664 Van Eck, J. (2010). Setaria viridis: a model for C4 photosynthesis. Plant Cell *22*, 2537-2544.
665 Bushnell, B. (2016). BBMap short read aligner. University of California, Berkeley, California URL
666 http://sourceforge net/projects/bbmap.
667 Calixto, C.P., Waugh, R., and Brown, J.W. (2015). Evolutionary relationships among barley and
668 Arabidopsis core circadian clock and clock-associated genes. J Mol Evol *80*, 108-119.
669 Covington, M.F., Maloof, J.N., Straume, M., Kay, S.A., and Harmer, S.L. (2008). Global
670 transcriptome analysis reveals circadian regulation of key pathways in plant growth and
671 development. Genome Biol *9*, R130.
672 Covington, M.F., Panda, S., Liu, X.L., Strayer, C.A., Wagner, D.R., and Kay, S.A. (2001). ELF3
673 modulates resetting of the circadian clock in Arabidopsis. Plant Cell *13*, 1305-1315.
674 Dixon, L.E., Knox, K., Kozma-Bognar, L., Southern, M.M., Pokhilko, A., and Millar, A.J. (2011).
675 Temporal repression of core circadian genes is mediated through EARLY FLOWERING 3 in
676 Arabidopsis. Curr Biol *21*, 120-125.
677 Dodd, A.N., Salathia, N., Hall, A., Kevei, E., Toth, R., Nagy, F., Hibberd, J.M., Millar, A.J., and
678 Webb, A.A. (2005). Plant circadian clocks increase photosynthesis, growth, survival, and
679 competitive advantage. Science *309*, 630-633.
680 Doherty, C.J., and Kay, S.A. (2010). Circadian control of global gene expression patterns. Annu
681 Rev Genet *44*, 419-444.
682 Doyle, M.R., Davis, S.J., Bastow, R.M., McWatters, H.G., Kozma-Bognar, L., Nagy, F., Millar, A.J.,
683 and Amasino, R.M. (2002). The ELF4 gene controls circadian rhythms and flowering time in
684 Arabidopsis thaliana. Nature *419*, 74-77.
685 Edelstein, A., Amodaj, N., Hoover, K., Vale, R., and Stuurman, N. (2010). Computer control of
686 microscopes using microManager. Curr Protoc Mol Biol *Chapter 14*, Unit14 20.
687 Edelstein, A.D., Tsuchida, M.A., Amodaj, N., Pinkard, H., Vale, R.D., and Stuurman, N. (2014).
688 Advanced methods of microscope control using muManager software. J Biol Methods *1*.
689 Edgar, R., Domrachev, M., and Lash, A.E. (2002). Gene Expression Omnibus: NCBI gene
690 expression and hybridization array data repository. Nucleic Acids Res *30*, 207-210.
691 Edgar, R.S., Green, E.W., Zhao, Y., van Ooijen, G., Olmedo, M., Qin, X., Xu, Y., Pan, M.,
692 Valekunja, U.K., Feeney, K.A.*, et al.* (2012). Peroxiredoxins are conserved markers of circadian
693 rhythms. Nature *485*, 459-464.
694 Faure, S., Turner, A.S., Gruszka, D., Christodoulou, V., Davis, S.J., von Korff, M., and Laurie, D.A.
695 (2012). Mutation at the circadian clock gene EARLY MATURITY 8 adapts domesticated barley
696 (Hordeum vulgare) to short growing seasons. Proc Natl Acad Sci U S A *109*, 8328-8333.

Filichkin, S.A., Breton, G., Priest, H.D., Dharmawardhana, P., Jaiswal, P., Fox, S.E., Michael, T.P., Chory, J., Kay, S.A., and Mockler, T.C. (2011). Global profiling of rice and poplar transcriptomes highlights key conserved circadian-controlled pathways and cis-regulatory modules. PLoS One *6*, e16907.

Goodstein, D.M., Shu, S., Howson, R., Neupane, R., Hayes, R.D., Fazo, J., Mitros, T., Dirks, W., Hellsten, U., Putnam, N., *et al.* (2012). Phytozome: a comparative platform for green plant genomics. Nucleic Acids Res *40*, D1178-1186.

Gould, P.D., Diaz, P., Hogben, C., Kusakina, J., Salem, R., Hartwell, J., and Hall, A. (2009). Delayed fluorescence as a universal tool for the measurement of circadian rhythms in higher plants. Plant J *58*, 893-901.

Graf, A., Schlereth, A., Stitt, M., and Smith, A.M. (2010). Circadian control of carbohydrate availability for growth in Arabidopsis plants at night. Proc Natl Acad Sci U S A *107*, 9458-9463.

Greenham, K., and McClung, C.R. (2015). Integrating circadian dynamics with physiological processes in plants. Nat Rev Genet *16*, 598-610.

Harmer, S.L. (2009). The circadian system in higher plants. Annu Rev Plant Biol *60*, 357-377.

Harmer, S.L., Hogenesch, J.B., Straume, M., Chang, H.S., Han, B., Zhu, T., Wang, X., Kreps, J.A., and Kay, S.A. (2000). Orchestrated transcription of key pathways in Arabidopsis by the circadian clock. Science *290*, 2110-2113.

Hazen, S.P., Schultz, T.F., Pruneda-Paz, J.L., Borevitz, J.O., Ecker, J.R., and Kay, S.A. (2005). LUX ARRHYTHMO encodes a Myb domain protein essential for circadian rhythms. Proc Natl Acad Sci U S A *102*, 10387-10392.

Helfer, A., Nusinow, D.A., Chow, B.Y., Gehrke, A.R., Bulyk, M.L., and Kay, S.A. (2011). LUX ARRHYTHMO encodes a nighttime repressor of circadian gene expression in the Arabidopsis core clock. Curr Biol *21*, 126-133.

Herrero, E., Kolmos, E., Bujdoso, N., Yuan, Y., Wang, M., Berns, M.C., Uhlworm, H., Coupland, G., Saini, R., Jaskolski, M., *et al.* (2012). EARLY FLOWERING4 recruitment of EARLY FLOWERING3 in the nucleus sustains the Arabidopsis circadian clock. Plant Cell *24*, 428-443.

Hicks, K.A., Albertson, T.M., and Wagner, D.R. (2001). EARLY FLOWERING3 encodes a novel protein that regulates circadian clock function and flowering in Arabidopsis. Plant Cell *13*, 1281-1292.

Hicks, K.A., Millar, A.J., Carre, I.A., Somers, D.E., Straume, M., Meeks-Wagner, D.R., and Kay, S.A. (1996). Conditional circadian dysfunction of the Arabidopsis early-flowering 3 mutant. Science *274*, 790-792.

Higgins, J.A., Bailey, P.C., and Laurie, D.A. (2010). Comparative genomics of flowering time pathways using Brachypodium distachyon as a model for the temperate grasses. PLoS One *5*, e10065.

Hsu, P.Y., and Harmer, S.L. (2014). Wheels within wheels: the plant circadian system. Trends in plant science *19*, 240-249.

Huang, H., Alvarez, S., Bindbeutel, R., Shen, Z., Naldrett, M.J., Evans, B.S., Briggs, S.P., Hicks, L.M., Kay, S.A., and Nusinow, D.A. (2016a). Identification of Evening Complex Associated Proteins in Arabidopsis by Affinity Purification and Mass Spectrometry. Mol Cell Proteomics *15*, 201-217.

739 Huang, H., Alvarez, S., and Nusinow, D.A. (2016b). Data on the identification of protein
740 interactors with the Evening Complex and PCH1 in Arabidopsis using tandem affinity
741 purification and mass spectrometry (TAP-MS). Data Brief *8*, 56-60.
742 Huang, H., and Nusinow, D. (2016a). Tandem Purification of His6-3x FLAG Tagged Proteins for
743 Mass Spectrometry from Arabidopsis. Bio-Protocol *6*.
744 Huang, H., and Nusinow, D.A. (2016b). Into the Evening: Complex Interactions in the
745 Arabidopsis Circadian Clock. Trends Genet *32*, 674-686.
746 Huang, H., Yoo, C.Y., Bindbeutel, R., Goldsworthy, J., Tielking, A., Alvarez, S., Naldrett, M.J.,
747 Evans, B.S., Chen, M., and Nusinow, D.A. (2016c). PCH1 integrates circadian and light-signaling
748 pathways to control photoperiod-responsive growth in Arabidopsis. eLife *5*, e13292.
749 Hughes, M.E., Hogenesch, J.B., and Kornacker, K. (2010). JTK_CYCLE: an efficient nonparametric
750 algorithm for detecting rhythmic components in genome-scale data sets. J Biol Rhythms *25*,
751 372-380.
752 Keller, A., Nesvizhskii, A.I., Kolker, E., and Aebersold, R. (2002). Empirical Statistical Model To
753 Estimate the Accuracy of Peptide Identifications Made by MS/MS and Database Search.
754 Analytical Chemistry *74*, 5383-5392.
755 Khan, S., Rowe, S.C., and Harmon, F.G. (2010). Coordination of the maize transcriptome by a
756 conserved circadian clock. BMC Plant Biol *10*, 126.
757 Khanna, R., Kikis, E.A., and Quail, P.H. (2003). EARLY FLOWERING 4 functions in phytochrome B-
758 regulated seedling de-etiolation. Plant Physiol *133*, 1530-1538.
759 Kim, W.Y., Hicks, K.A., and Somers, D.E. (2005). Independent roles for EARLY FLOWERING 3 and
760 ZEITLUPE in the control of circadian timing, hypocotyl length, and flowering time. Plant Physiol
761 *139*, 1557-1569.
762 Kolmos, E., Herrero, E., Bujdoso, N., Millar, A.J., Toth, R., Gyula, P., Nagy, F., and Davis, S.J.
763 (2011). A reduced-function allele reveals that EARLY FLOWERING3 repressive action on the
764 circadian clock is modulated by phytochrome signals in Arabidopsis. Plant Cell *23*, 3230-3246.
765 Kumar, R., Ichihashi, Y., Kimura, S., Chitwood, D.H., Headland, L.R., Peng, J., Maloof, J.N., and
766 Sinha, N.R. (2012). A High-Throughput Method for Illumina RNA-Seq Library Preparation. Front
767 Plant Sci *3*, 202.
768 Liu, X.L., Covington, M.F., Fankhauser, C., Chory, J., and Wagner, D.R. (2001). ELF3 encodes a
769 circadian clock-regulated nuclear protein that functions in an Arabidopsis PHYB signal
770 transduction pathway. Plant Cell *13*, 1293-1304.
771 Lou, P., Wu, J., Cheng, F., Cressman, L.G., Wang, X., and McClung, C.R. (2012). Preferential
772 retention of circadian clock genes during diploidization following whole genome triplication in
773 Brassica rapa. Plant Cell *24*, 2415-2426.
774 Lu, S., Zhao, X., Hu, Y., Liu, S., Nan, H., Li, X., Fang, C., Cao, D., Shi, X., Kong, L., *et al.* (2017).
775 Natural variation at the soybean J locus improves adaptation to the tropics and enhances yield.
776 Nat Genet.
777 Matos, D.A., Cole, B.J., Whitney, I.P., MacKinnon, K.J., Kay, S.A., and Hazen, S.P. (2014). Daily
778 changes in temperature, not the circadian clock, regulate growth rate in Brachypodium
779 distachyon. PLoS One *9*, e100072.

780 Matsubara, K., Ogiso-Tanaka, E., Hori, K., Ebana, K., Ando, T., and Yano, M. (2012). Natural
781 variation in Hd17, a homolog of Arabidopsis ELF3 that is involved in rice photoperiodic
782 flowering. Plant Cell Physiol *53*, 709-716.
783 McClung, C.R. (2013). Beyond Arabidopsis: the circadian clock in non-model plant species.
784 Semin Cell Dev Biol *24*, 430-436.
785 Michael, T.P., Mockler, T.C., Breton, G., McEntee, C., and Byer, A. (2008). Network discovery
786 pipeline elucidates conserved time-of-day-specific cis-regulatory modules. PLoS genetics.
787 Michael, T.P., Salome, P.A., and McClung, C.R. (2003). Two Arabidopsis circadian oscillators can
788 be distinguished by differential temperature sensitivity. Proc Natl Acad Sci U S A *100*, 6878-
789 6883.
790 Mizuno, T., Nomoto, Y., Oka, H., Kitayama, M., Takeuchi, A., Tsubouchi, M., and Yamashino, T.
791 (2014). Ambient temperature signal feeds into the circadian clock transcriptional circuitry
792 through the EC night-time repressor in Arabidopsis thaliana. Plant Cell Physiol *55*, 958-976.
793 Mockler, T.C., Michael, T.P., Priest, H.D., Shen, R., Sullivan, C.M., Givan, S.A., McEntee, C., Kay,
794 S.A., and Chory, J. (2007). The DIURNAL project: DIURNAL and circadian expression profiling,
795 model-based pattern matching, and promoter analysis. Cold Spring Harb Symp Quant Biol *72*,
796 353-363.
797 Murakami, M., Ashikari, M., Miura, K., Yamashino, T., and Mizuno, T. (2003). The Evolutionarily
798 Conserved OsPRR Quintet: Rice Pseudo-Response Regulators Implicated in Circadian Rhythm.
799 Plant and Cell Physiology *44*, 1229-1236.
800 Nagel, D.H., and Kay, S.A. (2012). Complexity in the wiring and regulation of plant circadian
801 networks. Curr Biol *22*, R648-657.
802 Nesvizhskii, A.I., Keller, A., Kolker, E., and Aebersold, R. (2003). A Statistical Model for
803 Identifying Proteins by Tandem Mass Spectrometry. Analytical Chemistry *75*, 4646-4658.
804 Nozue, K., Covington, M.F., Duek, P.D., Lorrain, S., Fankhauser, C., Harmer, S.L., and Maloof, J.N.
805 (2007). Rhythmic growth explained by coincidence between internal and external cues. Nature
806 *448*, 358-361.
807 Nusinow, D.A., Helfer, A., Hamilton, E.E., King, J.J., Imaizumi, T., Schultz, T.F., Farre, E.M., and
808 Kay, S.A. (2011). The ELF4-ELF3-LUX complex links the circadian clock to diurnal control of
809 hypocotyl growth. Nature *475*, 398-402.
810 Onai, K., and Ishiura, M. (2005). PHYTOCLOCK 1 encoding a novel GARP protein essential for the
811 Arabidopsis circadian clock. Genes Cells *10*, 963-972.
812 Ouyang, Y., Andersson, C.R., Kondo, T., Golden, S.S., and Johnson, C.H. (1998). Resonating
813 circadian clocks enhance fitness in cyanobacteria. Proc Natl Acad Sci U S A *95*, 8660-8664.
814 Plautz, J.D., Straume, M., Stanewsky, R., Jamison, C.F., Brandes, C., Dowse, H.B., Hall, J.C., and
815 Kay, S.A. (1997). Quantitative Analysis of Drosophila period Gene Transcription in Living
816 Animals. Journal of Biological Rhythms *12*, 204-217.
817 Poire, R., Wiese-Klinkenberg, A., Parent, B., Mielewczik, M., Schurr, U., Tardieu, F., and Walter,
818 A. (2010). Diel time-courses of leaf growth in monocot and dicot species: endogenous rhythms
819 and temperature effects. J Exp Bot *61*, 1751-1759.

Pokhilko, A., Fernandez, A.P., Edwards, K.D., Southern, M.M., Halliday, K.J., and Millar, A.J. (2012). The clock gene circuit in Arabidopsis includes a repressilator with additional feedback loops. Mol Syst Biol *8*, 574.

Pruneda-Paz, J.L., Breton, G., Para, A., and Kay, S.A. (2009). A functional genomics approach reveals CHE as a component of the Arabidopsis circadian clock. Science *323*, 1481-1485.

Saito, H., Ogiso-Tanaka, E., Okumoto, Y., Yoshitake, Y., Izumi, H., Yokoo, T., Matsubara, K., Hori, K., Yano, M., Inoue, H., *et al.* (2012). Ef7 encodes an ELF3-like protein and promotes rice flowering by negatively regulating the floral repressor gene Ghd7 under both short- and long-day conditions. Plant Cell Physiol *53*, 717-728.

Sakuraba, Y., Han, S.H., Yang, H.J., Piao, W., and Paek, N.C. (2016). Mutation of Rice Early Flowering3.1 (OsELF3.1) delays leaf senescence in rice. Plant Mol Biol.

Sakuraba, Y., Jeong, J., Kang, M.Y., Kim, J., Paek, N.C., and Choi, G. (2014). Phytochrome-interacting transcription factors PIF4 and PIF5 induce leaf senescence in Arabidopsis. Nat Commun *5*, 4636.

Schneider, C.A., Rasband, W.S., and Eliceiri, K.W. (2012). NIH Image to ImageJ: 25 years of image analysis. Nat Meth *9*, 671-675.

Shor, E., and Green, R.M. (2016). The Impact of Domestication on the Circadian Clock. Trends Plant Sci *21*, 281-283.

Sievers, F., Wilm, A., Dineen, D., Gibson, T.J., Karplus, K., Li, W., Lopez, R., McWilliam, H., Remmert, M., Soding, J., *et al.* (2011). Fast, scalable generation of high-quality protein multiple sequence alignments using Clustal Omega. Mol Syst Biol *7*, 539.

Song, Y.H., Ito, S., and Imaizumi, T. (2010). Similarities in the circadian clock and photoperiodism in plants. Curr Opin Plant Biol *13*, 594-603.

Song, Y.H., Shim, J.S., Kinmonth-Schultz, H.A., and Imaizumi, T. (2014). Photoperiodic Flowering: Time Measurement Mechanisms in Leaves. Annu Rev Plant Biol.

Van Leene, J., Eeckhout, D., Cannoot, B., De Winne, N., Persiau, G., Van De Slijke, E., Vercruysse, L., Dedecker, M., Verkest, A., Vandepoele, K., *et al.* (2015). An improved toolbox to unravel the plant cellular machinery by tandem affinity purification of Arabidopsis protein complexes. Nat Protocols *10*, 169-187.

Vizcaino, J.A., Deutsch, E.W., Wang, R., Csordas, A., Reisinger, F., Rios, D., Dianes, J.A., Sun, Z., Farrah, T., Bandeira, N., *et al.* (2014). ProteomeXchange provides globally coordinated proteomics data submission and dissemination. Nat Biotechnol *32*, 223-226.

Wang, L., Si, Y., Dedow, L.K., Shao, Y., Liu, P., and Brutnell, T.P. (2011a). A low-cost library construction protocol and data analysis pipeline for Illumina-based strand-specific multiplex RNA-seq. PLoS One *6*, e26426.

Wang, W., Barnaby, J.Y., Tada, Y., Li, H., Tor, M., Caldelari, D., Lee, D.U., Fu, X.D., and Dong, X. (2011b). Timing of plant immune responses by a central circadian regulator. Nature *470*, 110-114.

Wang, Z., Casas-Mollano, J.A., Xu, J., Riethoven, J.J., Zhang, C., and Cerutti, H. (2015). Osmotic stress induces phosphorylation of histone H3 at threonine 3 in pericentromeric regions of Arabidopsis thaliana. Proc Natl Acad Sci U S A *112*, 8487-8492.

Weller, J.L., Liew, L.C., Hecht, V.F.G., Rajandran, V., Laurie, R.E., Ridge, S., Wenden, B., Vander Schoor, J.K., Jaminon, O., Blassiau, C., *et al.* (2012). A conserved molecular basis for photoperiod adaptation in two temperate legumes. Proc Natl Acad Sci U S A *109*, 21158-21163.

Wijnen, H., and Young, M.W. (2006). Interplay of circadian clocks and metabolic rhythms. Annu Rev Genet *40*, 409-448.

Woelfle, M.A., Ouyang, Y., Phanvijhitsiri, K., and Johnson, C.H. (2004). The adaptive value of circadian clocks: an experimental assessment in cyanobacteria. Curr Biol *14*, 1481-1486.

Wu, J.F., Wang, Y., and Wu, S.H. (2008). Two new clock proteins, LWD1 and LWD2, regulate Arabidopsis photoperiodic flowering. Plant Physiol *148*, 948-959.

Yang, Y., Peng, Q., Chen, G.-X., Li, X.-H., and Wu, C.-Y. (2013). OsELF3 is involved in circadian clock regulation for promoting flowering under long-day conditions in rice. Mol Plant *6*, 202-215.

Yu, J.W., Rubio, V., Lee, N.Y., Bai, S., Lee, S.Y., Kim, S.S., Liu, L., Zhang, Y., Irigoyen, M.L., Sullivan, J.A., *et al.* (2008). COP1 and ELF3 control circadian function and photoperiodic flowering by regulating GI stability. Mol Cell *32*, 617-630.

Zagotta, M., Shannon, S., Jacobs, C., and Meeks-Wagner, D. (1992). Early-Flowering Mutants of *Arabidopsis thaliana*. Functional Plant Biology *19*, 411-418.

Zakhrabekova, S., Gough, S.P., Braumann, I., Muller, A.H., Lundqvist, J., Ahmann, K., Dockter, C., Matyszczak, I., Kurowska, M., Druka, A., *et al.* (2012). Induced mutations in circadian clock regulator Mat-a facilitated short-season adaptation and range extension in cultivated barley. Proc Natl Acad Sci U S A *109*, 4326-4331.

Zhang, X., Henriques, R., Lin, S.-S., Niu, Q.-W., and Chua, N.-H. (2006). Agrobacterium-mediated transformation of Arabidopsis thaliana using the floral dip method. Nat Protocols *1*, 641-646.

Zhao, J., Huang, X., Ouyang, X., Chen, W., Du, A., Zhu, L., Wang, S., Deng, X.W., and Li, S. (2012). OsELF3-1, an ortholog of Arabidopsis early flowering 3, regulates rice circadian rhythm and photoperiodic flowering. PLoS One *7*, e43705.

Zhu, D., Maier, A., Lee, J.H., Laubinger, S., Saijo, Y., Wang, H., Qu, L.J., Hoecker, U., and Deng, X.W. (2008). Biochemical characterization of Arabidopsis complexes containing CONSTITUTIVELY PHOTOMORPHOGENIC1 and SUPPRESSOR OF PHYA proteins in light control of plant development. Plant Cell *20*, 2307-2323.

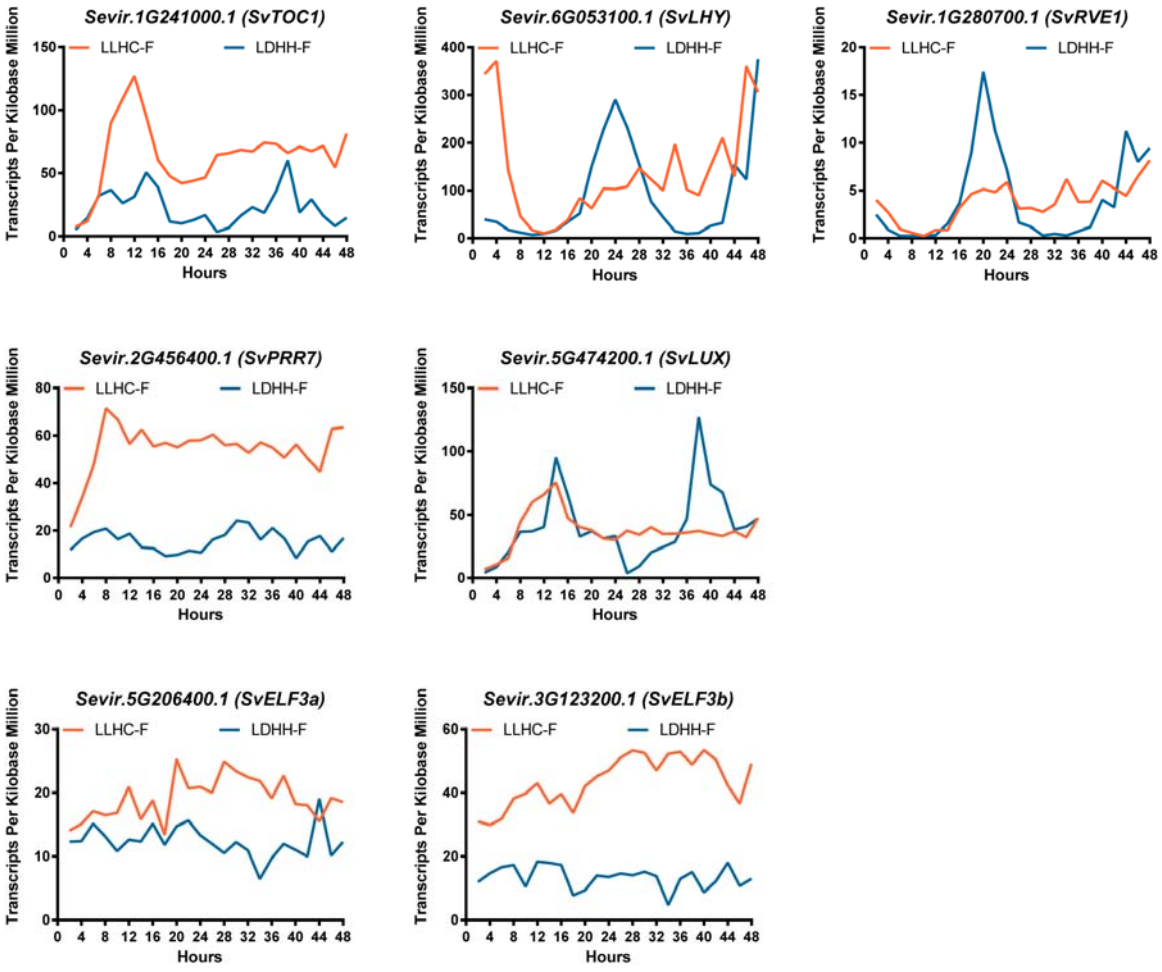

Figure 1. Circadian expression profiles of putative *S. viridis* clock components from Diel Explorer using time-course RNA-seq data. *S. viridis* plants were entrained by either photocycle (LDHH) or thermocycle (LLHC), followed by being sampled every 2 hours for 48 hours under constant temperature and light conditions (Free-Running; F) to generate time-course RNA-seq data. Mean values of Transcripts per Kilobase Million (TPM) from two experimental replicates for each timepoints per gene were plotted.

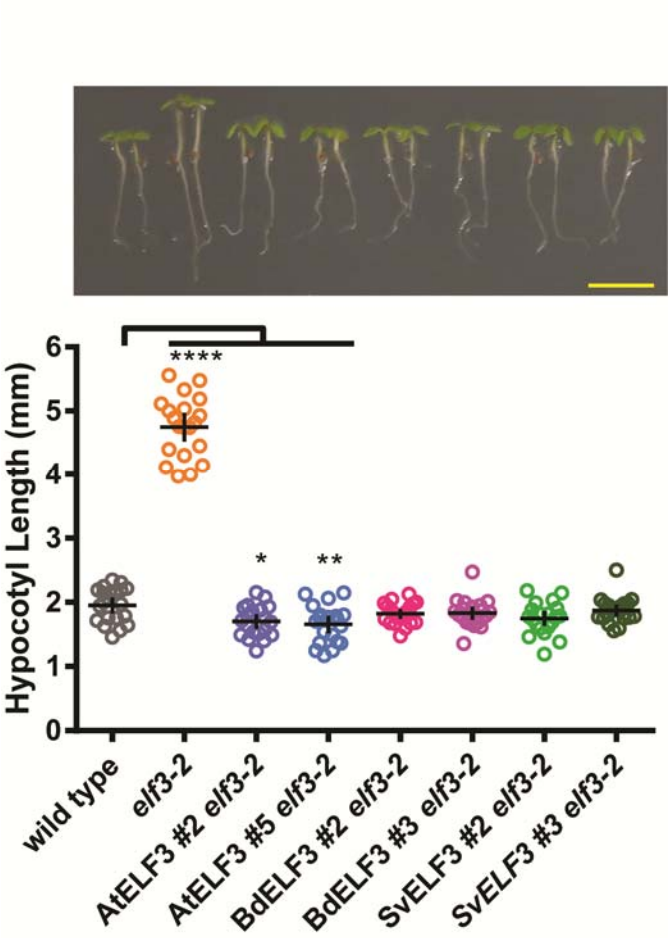

Figure 2. ELF3 orthologs suppress hypocotyl elongation defects in *elf3-2*. The hypocotyls of 20 seedlings of wild type, *elf3-2* mutant, AtELF3 *elf3-2*, BdELF3 *elf3-2*, and SvELF3 *elf3-2* (two independent transgenic lines for each ELF3 ortholog) were measured at 4 days after germination under 12-hour light :12-hour dark growth conditions at 22 ˚C. Upper panel shows representative seedlings of each genotype, with scale bar equal to 5 mm. Mean and 95% confidence intervals are plotted as crosshairs. This experiment was repeated three times with similar results. ANOVA analysis with Bonferroni correction was used to generate adjusted P values, * < 0.05, ** < 0.01, **** < 0.0001.

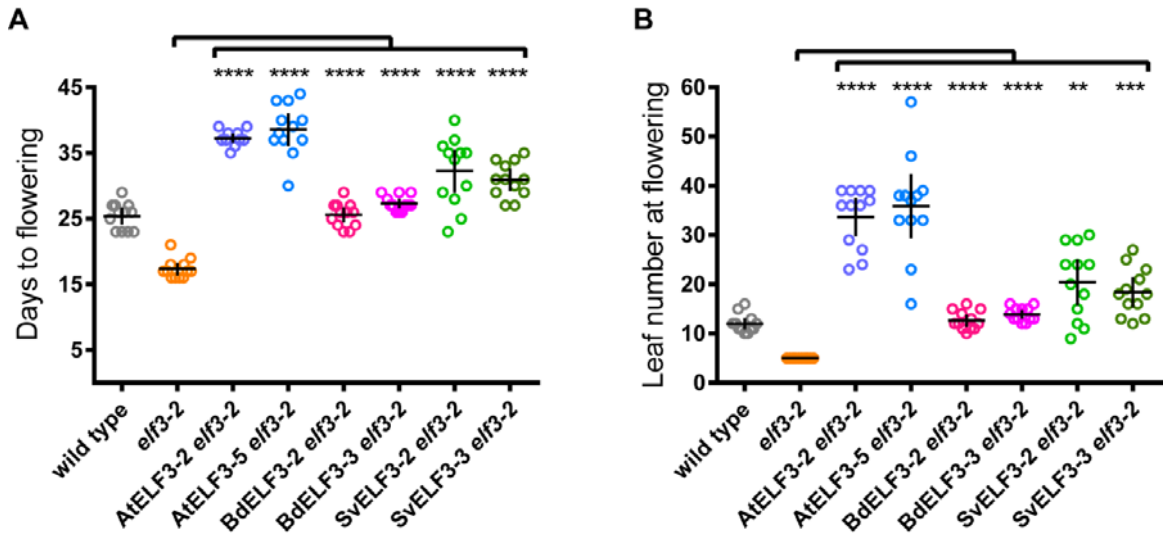

Figure 3. ELF3 orthologs suppress time to flowering of *elf3-2*. 12 wild type, *elf3-2* mutant, AtELF3 *elf3-2*, BdELF3 *elf3-2*, and SvELF3 *elf3-2* seedlings from two independent transformations were measured for days **(A)** and number of rosette leaves **(B)** at flowering (1 cm inflorescence). Mean and 95% confidence intervals are plotted as crosshairs. This experiment was repeated twice with similar results. ANOVA analysis with Bonferroni correction was used to generate adjusted P values, ** < 0.01, *** < 0.001, **** < 0.0001, of measurements when compared to the *elf3-2* mutant line.

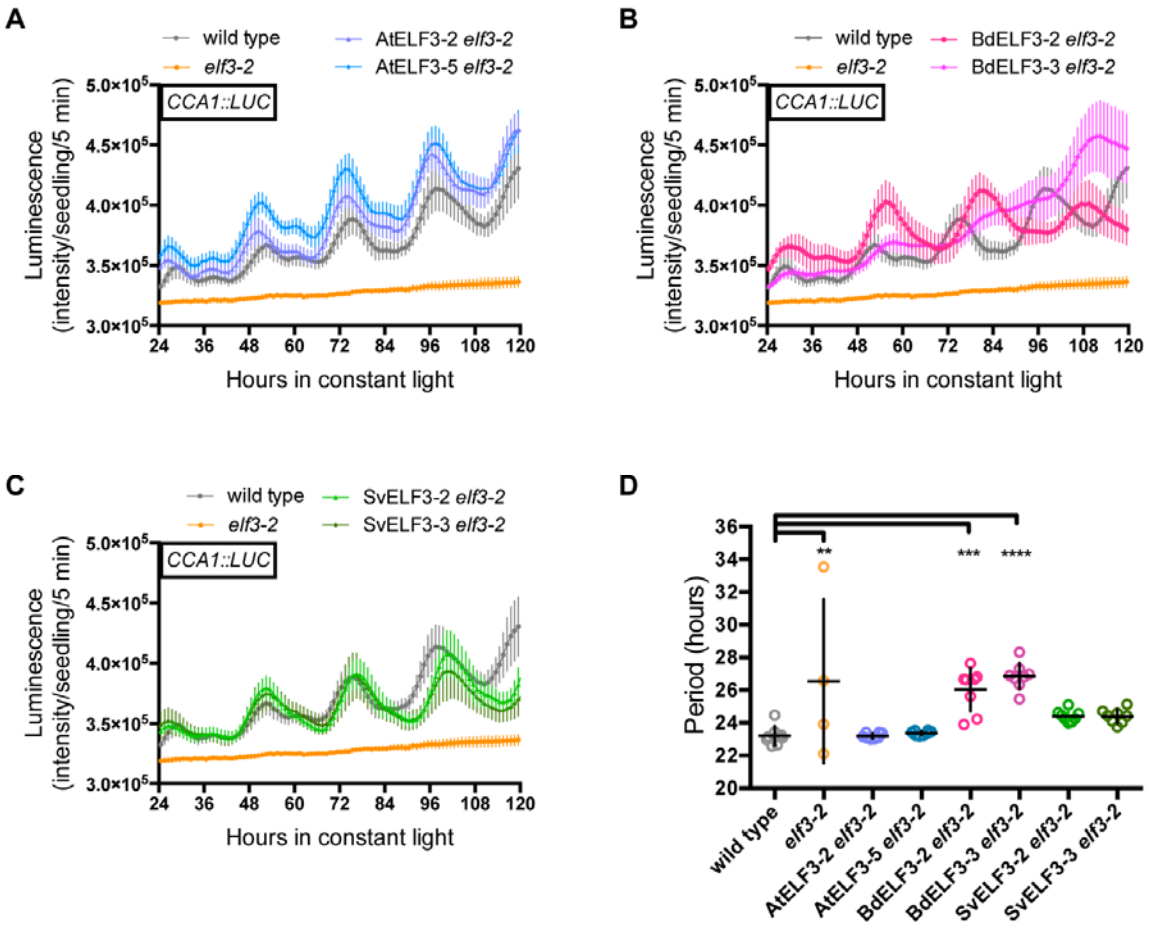

Figure 4. ELF3 orthologs can recover *CCA1::LUC* rhythms and amplitude in *elf3-2* mutants. 8 seedlings of wild type, *elf3-2* mutant, AtELF3 *elf3-2* **(A)**, BdELF3 *elf3-2* **(B)**, and SvELF3 *elf3-2* **(C)** from two independent transformations were imaged for bioluminescence under constant light after entrainment in 12-hour light :12-hour dark growth conditions at 22 ˚C. Each plot shows average bioluminescence of all seedlings along with 95% confidence interval (error bars). This experiment was repeated twice with similar results. Note that wild type and *elf3-2* mutant data was plotted on all graphs for comparison. **(D)** Periods of seedlings. Only periods with a Relative Amplitude Error below 0.5 (see Supplemental Figure 7) were plotted. Mean and 95% confidence intervals are plotted as crosshairs. ANOVA analysis with Bonferroni correction was used to generate adjusted P values, ** < 0.01, *** < 0.001, **** < 0.0001, of measurements when compared to the wild type.

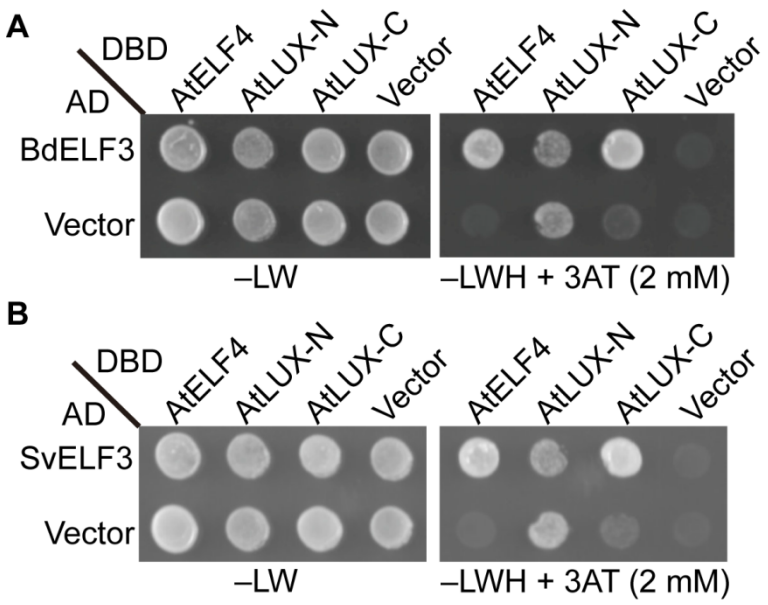

Figure 5. Both BdELF3 and SvELF3 can directly bind to AtELF4 and AtLUX. Yeast two-hybrid analysis of testing if either BdELF3 **(A)** or SvELF3 **(B)** can directly interact with either AtELF4, the N-terminal half of AtLUX (AtLUX-N, a.a. 1-143) or the C-terminal half of AtLUX (AtLUX-C, a.a. 144-324). –LW tests for the presence of both bait (DBD) and pray (AD) vectors, while the –LWH + 3AT tests for interaction. Vector alone serves as interaction control. This experiment was repeated twice with similar results.